Monodromy in systems with coupled angular momenta and rearrangement of bands in quantum spectra

L. Grondin, D. A. Sadovskií, and B. I. Zhilinskií*

Université du Littoral,UMR CNRS 8101, Boîte Postale 5526, 59379 Dunkerque Cedex, France

(Dated: April 2001, final, printed: July 19, 2001; revised 11/4/01)

We continue to study the relation between the redistribution of levels in quantum energy spectra and monodromy of the corresponding classical system [see Phys. Lett. A **256** 235 (1999)]. The system with two coupled angular momenta and SO(2) symmetry is compared to the system with three momenta and SO(3) symmetry.

PACS numbers: 03.65.Sq, 32.30.-r, 33.20.Wr

I. INTRODUCTION

Redistribution of quantum energy levels between different energy spectrum branches which occurs when parameters of the system, such as the value of an integral of motion, are varied [1] was recently shown to be related to classical monodromy [2] and to the existence and modification of topological quantum numbers [3]. The study in [1–3] focused on a very simple model system with two coupled angular momenta $\mathbf{L}_1$ and $\mathbf{L}_2$ invariant with respect to the SO(2) symmetry group (Fig. 1, left). For brevity we will refer to this system as $2\mathbf{L}|_{\mathrm{SO}(2)}$. The recent developments [2, 3] are of considerable general interest: on the one hand, systems of this kind emerge in numerous problems of atomic, molecular, nuclear, and even solid state physics, and on the other hand, we can now analyze, classify, and describe all such systems using universal fundamental mathematical concepts of classical monodromy and Chern indices.

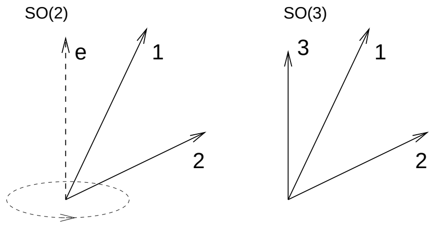

FIG. 1: Two vectors (angular momenta) in the presence of axial symmetry SO(2) whose axis is given by the unit vector **e**, and three vectors in the presence of SO(3).

One of the most widely known two-momentum systems is, of course, the hydrogen atom. Neglecting spin, it can be considered as a two-body Kepler problem and described in terms of two angular momenta of equal fixed amplitude. Certain perturbations of the hydrogen atom, notably by one external electric or magnetic field, two parallel, or two orthogonal fields, lower continuous symmetry of the system to SO(2) and couple the two momenta. Furthermore, as has been shown recently in Ref. [4], the classical orthogonal field system has monodromy (in a certain interval of the field strength ratio).

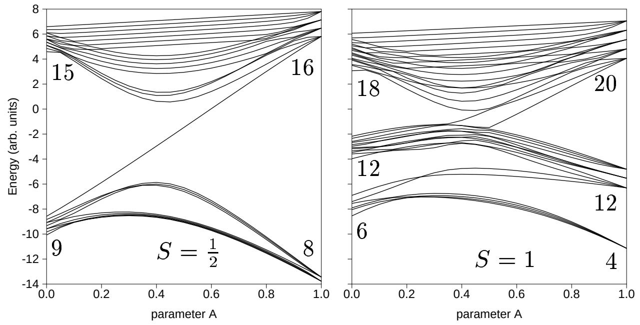

FIG. 2: Correlation diagrams of simple $3\mathbf{L}|_{\mathrm{SO}(3)}$ systems with $I = \frac{3}{2}$, $L = 1$, $S = \frac{1}{2}$ (left), and $S = 1$ (right) described by Hamiltonian (1). The number of states in the limit $a = 0$ and $a = 1$ is indicated for each multiplet (band).

As a simple example of a three-momentum system consider the hyperfine structure in a hypothetical family of atomic states described by the Hamiltonian

$$H = a\,\mathbf{SL} + (1-a)\mathbf{SI} + \gamma(2S_z + L_z), \qquad (1)$$

where the first and second terms have spherical symmetry SO(3) and represent coupling of electron spin **S** (for a one-electron atom $S = \frac{1}{2}$) with orbital angular momentum **L** and nuclear spin **I** respectively. We add an axially symmetric perturbation due to a weak external magnetic field γ in order to uncover the degeneracy of quantum states. The value of parameter a characterizes different members of the family, we use $0 \le a \le 1$ while $\gamma \ll 1$. In the "usual" limit of $a \approx 1$, the energy level system consists of multiplets labeled by the good quantum number $J = |L-S|, \ldots, L+S$ of the angular momentum $\mathbf{J} = \mathbf{S} + \mathbf{L}$. In the limit $a \approx 0$ the multiplets are labeled by $F = |I-S|, \ldots, I+S$. In the intermediate case, where the hyperfine and spin-orbit interactions are comparable, the structure is complicated.

The energy level spectrum of the Hamiltonian (1) is plotted in Fig. 2. It consists of groups of levels or multiplets. The number of states in the multiplet equals $(2J+1)(2I+1)$ and $(2F+1)(2L+1)$ in the respective limit of $a \approx 1$ and $a \approx 0$, these states are split due to the small Zeeman perturbation. Generally, the numbers in the two limits cannot match and some sort of redistribution of levels should occur when we change a. Thus, in the $S=\frac{1}{2}$ example, one level is redistributed. Atomic states with comparable hyperfine and spin-orbit contributions have been known since early 30-s [5]. Their structure is, of course, more complicated than our simple model. This model only suggests the way to find the similarities between individual states characterized by particular values of $\mathbf{S}$, $\mathbf{L}$, and $\mathbf{I}$.

It is quite typical for many-body systems to have two different degrees of freedom, a "slow" and a "fast" degree, each ascribed an angular momentum of large and small amplitude respectively. In molecules these degrees can be associated with electron motion and vibration (vibronic system), vibration and rotation (rovibrational system, see examples in Refs. [6, 7]), electron motion or spin and rotation; in Rydberg atoms and molecules we also find that spin and electronic orbital motion can differ vastly in their time scales (spin-orbit systems); in nuclei the two degrees can be vibrations and rotations, and so on. Quantum energy levels of all such systems are grouped into "branches", "bands", multiplets, etc which can cross or exchange individual levels when parameters of the system vary. The most basic example of such phenomena was considered in [1]. It will be very interesting to understand fully the mathematical analogy between these phenomena and the topological quantum numbers used in the description of the quantum Hall effect [8].

The aim of this paper is to make another passage along the far fetched and difficult connection path from classical monodromy to topological quantum numbers in an attempt to advance concrete physical and mathematical understanding of a number of important aspects which remain presently at the level of intuition and hypothesis. Monodromy or, more generally, topological obstructions to global action-angle variables in classical Liouville integrable Hamiltonian systems [9] has been well understood only for the case of two degrees of freedom [10–12]. In fact all known examples of such obstructions and of the corresponding defect in the lattice of quantum energy levels [2, 4, 13–15] are of the simplest case known in two degrees of freedom. It should also be remarked in this context that classical integrability is not an absolutely necessary property of the systems we study but rather a simplifying factor. It has been suggested in [4] that monodromy can naturally extend to KAM-type systems and monodromy-like phenomena in non-integrable systems remain another open problem to tackle.

In order to understand certain aspects of systems with larger classical phase spaces we consider a system with three coupled constant amplitude angular momenta $3\mathbf{L}|_{\mathrm{SO}(3)}$, a simple generalization of $2\mathbf{L}|_{\mathrm{SO}(2)}$ in [1]. We make this three degrees of freedom system integrable by imposing SO(3) symmetry (Fig. 1, right) and then analyze the geometry of families of dynamically invariant subspaces using the methods of Refs. [2, 4, 10]. After reduction of symmetries, this study uncovers striking mathematical equivalence of the three momentum system $3\mathbf{L}|_{\mathrm{SO}(3)}$ and the $2\mathbf{L}|_{\mathrm{SO}(2)}$ system, and at the same time reveals important generic features of the multidimensional case.

II. SYSTEM WITH TWO COUPLED ANGULAR MOMENTA ($2\mathbf{L}|_{\mathrm{SO}(2)}$)

We begin with a brief review of the two-momentum system $2\mathbf{L}|_{\mathrm{SO}(2)}$ which serves as a framework to the rest of the paper where the analysis of the three-momentum system $3\mathbf{L}|_{\mathrm{SO}(3)}$ is detailed along similar lines.

A. Classical mechanical system

The $2\mathbf{L}|_{\mathrm{SO}(2)}$ system is a Hamiltonian dynamical system which can be described in terms of six dynamical variables $(\mathbf{L}_1)_i$ and $(\mathbf{L}_2)_i$, $i=1,2,3$, subject to two relations,

$$\mathbf{L}_1^2 = \sum (\mathbf{L}_1)_i = L_1^2, \quad \mathbf{L}_2^2 = \sum (\mathbf{L}_2)_i = L_2^2,$$

where the amplitudes L_1 and L_2 are fixed. It follows that the $2\mathbf{L}|_{\mathrm{SO}(2)}$ has two degrees of freedom, and the phase space of this system is the product of two spheres $S_2 \times S_2$. The six dynamical variables generate the Poisson algebra so(3) × so(3),

$$\{(\mathbf{L}_\alpha)_i, (\mathbf{L}_\beta)_j\} = \varepsilon_{ijk}\, \delta_{\alpha\beta}\, (\mathbf{L}_\alpha)_k,$$

and classical equations of motion represent, therefore, a system of two rotors. Due to the SO(2) symmetry, the $2\mathbf{L}|_{\mathrm{SO}(2)}$ system has an integral of motion

$$(\mathbf{J}\cdot\mathbf{e}) = J_e = (\mathbf{L}_1\cdot\mathbf{e}) + (\mathbf{L}_2\cdot\mathbf{e}),$$

which is the projection of the total angular momentum $\mathbf{L}_1+\mathbf{L}_2$ on the axis of symmetry. The system is, therefore, Liouville integrable and has the energy H and momentum $(\mathbf{J}\cdot\mathbf{e})$ as first integrals.

B. Invariants of the SO(2) action

Up to an arbitrary rotation about axis $\mathbf{e}$ a configuration of the two vectors $\mathbf{L}_1$ and $\mathbf{L}_2$ (see Fig. 1, left) can be characterized uniquely by the values of three functions

$$L_{1e} = (\mathbf{L}_1\cdot\mathbf{e}), \quad L_{2e} = (\mathbf{L}_2\cdot\mathbf{e}), \quad \xi = (\mathbf{L}_1\cdot\mathbf{L}_2), \tag{2a}$$

i.e., by three angles between $\mathbf{L}_1$, $\mathbf{L}_2$ and $\mathbf{e}$, and by the sign of the mixed product

$$\sigma = \big([\mathbf{L}_1\times\mathbf{L}_2]\cdot\mathbf{e}\big), \tag{2b}$$

which distinguishes "left" and "right" configurations. If we extend the SO(2) symmetry by adding a symmetry operation which changes the sign of the mixed product σ the latter will no longer be necessary since "left" and "right" orientations become equivalent. In the case of ordinary vectors the additional symmetry operation can be spatial inversion and the resulting group is O(2), in the case of angular momenta (which are inversion invariant) this operation can be time reversal $\mathcal{T}$ which results in simultaneous inversion of $\mathbf{L}_1$ and $\mathbf{L}_2$ or a combination of $\mathcal{T}$ with some spatial operation. The particular operation $\mathcal{T}_2$, which is a combination of $\mathcal{T}$ with a rotation by π about any axis orthogonal to $\mathbf{e}$, leaves all main invariants in Eq. (2a) unchanged while reversing the sign of σ in Eq. (2b). The resulting group $\mathrm{SO}(2) \wedge \mathcal{T}_2$ is isomorphic to spatial groups $C_{\infty v}$ and O(2). Any $\mathrm{SO}(2)\wedge\mathcal{T}_2$ invariant Hamiltonian can be written as a function of invariants in Eq. (2a), the particular $2\mathbf{L}|_{\mathrm{SO}(2)}$ Hamiltonian of Ref. [2] being

$$H_\gamma = \frac{1-\gamma}{L_1}(\mathbf{L}_1 \cdot \mathbf{e}) + \frac{\gamma}{L_1 L_2}(\mathbf{L}_1 \cdot \mathbf{L}_2), \quad 0 \le \gamma \le 1. \quad (3)$$

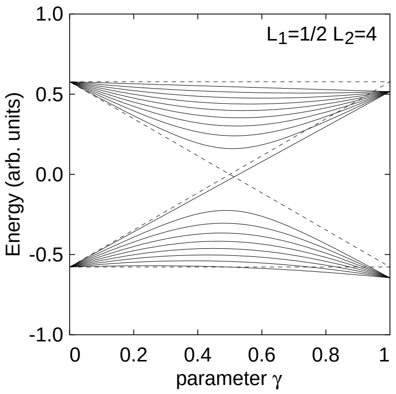

FIG. 3: Quantum energies (solid lines) and semi-quantum relative equilibria (dashed lines) of the two-momentum system $2\mathbf{L}|_{\mathrm{SO}(2)}$ with Hamiltonian (3), see Refs. [1, 2].

C. Quantum system. Energy level transfer

The quantum system $2\mathbf{L}|_{\mathrm{SO}(2)}$ is described in terms of operators $(\mathbf{L}_1)_s$ and $(\mathbf{L}_2)_s$, $s = 1, 2, 3$ [16], which obey commutation relations of so(3)×so(3)

$$(\mathbf{L}_\alpha)_a(\mathbf{L}_\beta)_b - (\mathbf{L}_\alpha)_b(\mathbf{L}_\beta)_a = i\,\varepsilon_{abc}\,\delta_{\alpha\beta}\,(\mathbf{L}_\alpha)_c.$$

The most elementary example of branches and level transfer can be obtained with Hamiltonian (3) in the case when "spin" $\mathbf{L}_1$ has the lowest nonzero quantum number $\frac{1}{2}$ and the mechanical momentum $\mathbf{L}_2$ (which can be associated with electronic or rotational motion) is large. At small γ we observe two groups of levels, or *bands*, which are distinguished by $l_1 = \pm\frac{1}{2}$ and which have $2l_2 + 1$ levels each. The two bands near the limit $\gamma \approx 1$ are labelled by quantum number $j = l_2 \pm \frac{1}{2}$ of the total angular momentum $\mathbf{L}_1 + \mathbf{L}_2$ and have $2l_2$ and $2l_2{+}2$ levels. Necessarily, one quantum level is redistributed between the bands when γ changes from 0 to 1. This transfer is illustrated in Fig. 3.

D. Complete analysis of classical system. Reduction

Classical system $2\mathbf{L}|_{\mathrm{SO}(2)}$ can be solved entirely using simple geometric methods. First the symmetry $\mathrm{SO}(2) \wedge \mathcal{T}_2$ is reduced using the theory of invariants. The reduced system has one degree of freedom. Then all constant level sets of the Hamiltonian H_γ on the reduced space of dimension 2 are classified according to their topology. This classification is trivialized by the fact that H_γ is a linear function of the $\mathrm{SO}(2) \wedge \mathcal{T}_2$ invariants in Eq. (2a) and its constant level sets are straight lines (or planes).

The action of SO(2) on the initial phase space $S_2 \times S_2$ is not free, there are four fixed points of this action which can be characterized using the values of invariants

$$(\mathbf{L}_1 \cdot \mathbf{e}) = \pm L_1, \quad (\mathbf{L}_2 \cdot \mathbf{e}) = \pm L_2,$$

or the critical values of the integral $(\mathbf{L}_1 + \mathbf{L}_2) \cdot \mathbf{e}$,

$$j = -L_1 - L_2,\ L_1 - L_2,\ L_2 - L_1,\ L_1 + L_2.$$

To remove such SO(2) symmetry we must use *singular* reduction. We use two variations of the latter, dynamical singular reduction and symmetry group reduction, which are both based on the invariant theory. Concrete examples can be found in Refs. [2, 4, 17], the book [10] and the recent review [18] give a more general discussion.

Pure symmetry group reduction aims at representing each orbit of the $\mathrm{SO}(2)\wedge\mathcal{T}_2$ action on $S_2 \times S_2$ as a point on the orbit space $\mathcal{O}$ of dimension 3. Dynamical reduction descends from $S_2 \times S_2$ to a phase space P_j (of dimension 2) constructed for each fixed value of the integral of motion. Each point on P_j lifts to an orbit of the flow of the vector field $X_{(\mathbf{L}_1+\mathbf{L}_2)\cdot\mathbf{e}}$. In other words, dynamical reduction is group reduction of the SO(2) action on the constant j slice of $S_2 \times S_2$. Symmetry group reduction gets rid of all symmetries (continuous, discrete, reversal) and gives the most concise representation of the reduced system. In fact, the orbit space $\mathcal{O}$ can be regarded as a continuous family (of the images of) the reduced phase spaces P_j. On the other hand, dynamical reduction should be used to study equations of motion of the reduced system.

In simple terms, reduction is done as follows. Consider generators in Eq. (2) of the ring of all polynomials in $(\mathbf{L}_\alpha)_i$ invariant with regard to the SO(2) (or $\mathrm{SO}(2) \wedge \mathcal{T}_2$) action. Two fundamental ideas are involved at this point. (i) The values of generators introduced in Eq. (2) can be used to label uniquely all orbits of the group action, so that these invariants can serve as nonlinear coordinates for the orbit space construction. (ii) Linearly independent generators are *not* algebraically independent, algebraic relation(s) between them or *sygyzies* together with inequalities restricting their possible values define the orbit spaces $\mathcal{O}$ and P_j as semi-algebraic varieties and thus characterize these spaces topologically. In the case of generators in Eq. (2) we have just one such relation,

$$\sigma^2 + (\xi - L_{1e}L_{2e})^2 - (L_1^2 - L_{1e}^2)(L_2^2 - L_{2e}^2) = 0, \quad (4)$$

as well as several obvious inequalities

$$\frac{|L_{1e}|}{L_1} \le 1, \quad \frac{|L_{2e}|}{L_2} \le 1, \quad \frac{|\xi|}{L_1L_2} \le 1, \quad \frac{|\sigma|}{L_1L_2} \le 1.$$

In order to reduce the $\mathcal{T}_2$ symmetry, we should also restrict $\sigma \ge 0$. In that case, the orbit space $\mathcal{O}$ can be represented as a closed 3-ball in the space R_3 with coordinates L_{1e}, L_{2e}, and ξ. The surface (the boundary) of this ball is defined by the equation

$$\sigma^2(L_{1e}, L_{2e}, \xi) = 0,$$

and looks like a tetrahedron with rounded edges and four singularities at the vertices which represent four fixed points of the $\mathrm{SO}(2) \wedge \mathcal{T}_2$ action on $S_2 \times S_2$ (see [2, 4, 17, 18]).

Cutting $\mathcal{O}$ by planes of constant $j = L_{1e} + L_{2e}$ gives images $P_j/\mathcal{T}_2$ of reduced phase spaces P_j; depending on j the space P_j can either be a point (for maximum and minimum $j = \pm(L_1+L_2)$), a smooth 2-sphere, or a *singular* space for $j = \pm(L_1 - L_2)$ which is a 2-sphere with one singular point on the surface. Intersections of planes of constant j with those of constant $H_\gamma(L_{1e}, L_{2e}, \xi) = h$ and with $\mathcal{O}$ are images of individual dynamically invariant subspaces of the $2\mathbf{L}|_{\mathrm{SO}(2)}$ system. In the original space $S_2 \times S_2$ these can be regular Liouville 2-tori $T_2(h, j)$, periodic orbits S_1 (relative equilibria), fixed points (elliptic equilibria), or a *pinched torus* (a homoclinic connection of stable and unstable manifolds of a hyperbolic equilibrium) shown in Fig. 4. This latter singular space exists for one of the special values of $j = \pm(L_1 - L_2)$ in an interval of the values of the parameter γ.

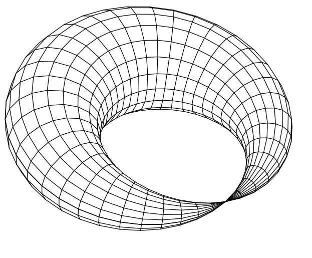

FIG. 4: Singly pinched 2-torus.

E. Correspondence of quantum and classical reduced systems

We give a simple topological characteristics of the family of reduced classical systems and corresponding quantum systems. To establish quantum-classical correspondence we prefer going from quantum to classical mechanics rather than discussing quantization of the classical system.

1 *Quantum multiplets of states with fixed J_e*

The total number of states in the quantum $2\mathbf{L}|_{\mathrm{SO}(2)}$ system equals $(2l_1+1)(2l_2+1)$. These states can be represented using basis functions $|l_1, m_1, l_2, m_2\rangle$ where projections m_1 and m_2 of $\mathbf{L}_1$ and $\mathbf{L}_2$ take integer or half integer values in the range $-l_1, \ldots, l_1$ and $-l_2, \ldots, l_2$ respectively [16]. To find the number of states $\mathcal{N}$ with given fixed projection j_e of the total angular momentum $\mathbf{J}$ we should count all possible pairs of (m_1, m_2) such that $j_e = m_1 + m_2$. Assuming $l_1 \ge l_2$, we distinguish three domains of the j_e values and find the number $\mathcal{N}$ in each domain,

$$\begin{aligned}
\mathcal{N} &= l_1 + l_2 - |j_e| + 1, \quad l_1 + l_2 \ge j_e \ge l_1 - l_2, \\
\mathcal{N} &= 2l_2 + 1, \quad |j_e| \le l_1 - l_2, \\
\mathcal{N} &= l_1 + l_2 - |j_e| + 1, \quad l_2 - l_1 \ge j_e \ge -l_1 - l_2.
\end{aligned}$$

As shown in Fig. 5, the function $\mathcal{N}(j_e)$ of the $2\mathbf{L}|_{\mathrm{SO}(2)}$ system is a piecewise linear continuous function of the momentum j_e which changes its slope at the critical values of j_e.

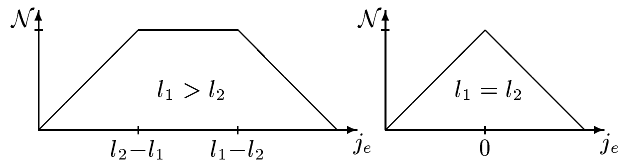

FIG. 5: Number of states diagram of the $2\mathbf{L}|_{\mathrm{SO}(2)}$ system.

2 *Number of states supported by the reduced phase space*

The diagram in Fig. 5 suggests an eloquent general characteristics of the continuous family of classical reduced systems labelled by the fixed value c of the momentum J_e. Classical interpretation of this diagram follows from the well-known semi-classical limit relation between the number of quantum states and the phase space volume accessible to the classical system, a basic relation in geometric quantization.

In the case of Euclidean geometry with s degrees of freedom and standard symplectic form $dq \wedge dp$ the volume element ΔV of the phase space equals, up to a factor, the number of states it supports,

$$\Delta\mathcal{N} = (2\pi\hbar)^{-s}\Delta q_1 \cdots \Delta q_s \Delta p_1 \cdots \Delta p_s$$

(see, for example, Chap. VII §49 of Ref. [19]). In general, relation between $\Delta\mathcal{N}$ and ΔV can be more complicated. Thus the phase space of a system with angular momentum $\mathbf{L}$ of constant amplitude L is a 2-sphere of radius L. In this case

$$\Delta\mathcal{N} = (2\pi L\hbar)^{-1}\Delta V.$$

The constant factor $1/L$ (the curvature) reflects the nonstandard Poisson bracket $\{L_x, L_y\} \approx L$ of the local symplectic coordinates on S_2^L. Using atomic units where $\hbar = 1$ and assuming $L \approx l + \frac{1}{2}$, we obtain that for the whole sphere S_2^L

$$\mathcal{N} = (2\pi L)^{-1}V = (2\pi L)^{-1}4\pi L^2 = 2L = 2l + 1.$$

In order to compute the number of states supported by the reduced phase space P_c of the $2\mathbf{L}|_{\mathrm{SO}(2)}$ system we recall that P_c is homologic to a 2-sphere. Moreover, as we show in the appendix, the phase space space P_c can be mapped to a sphere S_2 while the Poisson algebra of the reduced $2\mathbf{L}|_{\mathrm{SO}(2)}$ system can be simultaneously deformed into a standard Lie algebra so(3). Even though this map is (necessarily) singular at critical values of c, it preserves $\mathcal{N}$ because this latter characteristics is of topological nature. As shown in the appendix, the diameter of the S_2 image of P_c is defined exactly in the same way as the number of states $\mathcal{N}$ in the previous section and in Fig. 5. In fact, assuming $L_1 = l_1 + \frac{1}{2}$ and $L_2 = l_2 + \frac{1}{2}$ the two definitions match exactly.

3 Mathematical aspects

Relation of the band structure and the number of states of the quantum $2\mathbf{L}|_{\mathrm{SO}(2)}$ system to various characteristics of the corresponding classical mechanical system can be analyzed within a more formal mathematical framework. Figure 5 represents the Liouville volume of the reduced phase space P_c as function Ψ of the corresponding integral of motion c. By the theorem of Duistermaat-Heckman [20–22] $\Psi(c)$ is a piecewise linear function whose slope is given by the Chern class of the principle bundle. The values of the Chern class are defined by the group action on the initial phase space. In the $2\mathbf{L}|_{\mathrm{SO}(2)}$ case (with $l_1 > l_2$, the group SO(2) and phase space $S_2 \times S_2$) the values of the Chern class equal $+1$, 0, and -1 when $j_e < l_2 - l_1$, $l_2 - l_1 < j_e < l_1 - l_2$, and $j_e > l_1 - l_2$ respectively. In particular, this means that the total space of the bundle (the constant level set of j_e in $S_2 \times S_2$) has the topology of S_3, $S_1 \times S_2$, and S_3. Finally, the same Fig. 5 can be interpreted as a Delzant polytope associated to a symplectic manifold with a torus action defined on it [21].

Our present work remains at a more intuitive and descriptive level and leaves a comprehensive mathematical analysis of the above conjectures to future research. Understanding of deeper universal mathematical meaning of some of our concepts should be important to further generalizations and will undoubtedly improve translation between physical and mathematical descriptions.

F. Classical and quantum monodromy

The phenomenon of monodromy can be understood as soon as we describe how invariant dynamical subspaces, generically tori $T_2(h, j)$, *fit together*. To this end we use the results of the previous section to construct the energy-momentum map $\mathcal{EM}$,

$$\mathcal{EM} : S_2 \times S_2 \to R_2 : p \to \Big(H_\gamma(p), J_e(p)\Big) = (h, j),$$

which represents dynamically invariant subspaces of $S_2 \times S_2$ as points (h, j) of a 2-plane. The image of $\mathcal{EM}$ for the $2\mathbf{L}|_{\mathrm{SO}(2)}$ system is a closed region (disk) in R_2 (see figures in Ref. [2] and Fig. 6) with piecewise smooth borders. Singular points on its borders represent fixed points on $S_2 \times S_2$, other border points (h, j) lift to periodic orbits S_1 which have maximum and minimum j at given h. In the particular case shown in Fig. 6 all interior points *except one* lift to regular smooth 2-tori in $S_2 \times S_2$, the exceptional point is an isolated critical value $(h, j)_{\mathrm{crit}}$ of $\mathcal{EM}$ and the fiber $\mathcal{EM}^{-1}(h, j)_{\mathrm{crit}}$ is a singly pinched torus shown in Fig. 4.

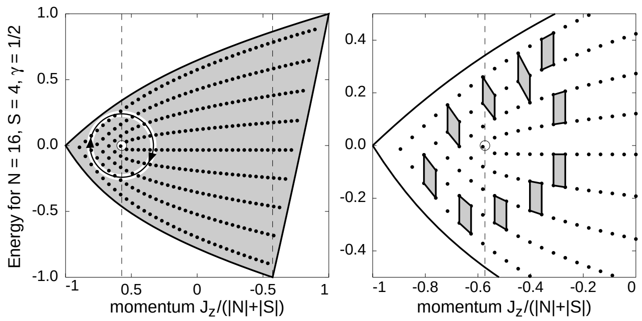

FIG. 6: The image of classical (shaded area and solid lines) and quantum (black dots) energy-momentum map $\mathcal{EM}$ in the case of the two-momentum system $2\mathbf{L}|_{\mathrm{SO}(2)}$ with monodromy. White circle represents the pinched torus, dashed lines mark critical values $\pm(L_1 - L_2)$ of momentum J_e. Adapted with permission from Ref. [2].

It is a theorem [11, 12, 23] that a (two degrees of freedom Hamiltonian integrable) system with such critical value of its energy-momentum map $\mathcal{EM}$ has *monodromy*. Monodromy means that such integrable system does not have global action-angle coordinates. Local action-angle coordinates define angle coordinates on all regular tori (h, j) in the neighborhood of a regular torus $(h, j)_0$, label such tori by the values of the two actions (j_1, j_2), and give a prescription on where to find the $\mathcal{EM}$ image of the torus $(j_1+\delta, j_2+\delta)$. This prescription is represented graphically in Fig. 6, right, as a small elementary cell in (the set of regular points of) the image of $\mathcal{EM}$. The shape of the cell defines uniquely how the cell can be moved to an adjacent cell. When we move our cell along a closed path in the set of regular values of $\mathcal{EM}$ encircling the image of the pinched torus $(h,j)_{\rm crit}$, the cell does not come to itself. This means that at least one of our actions (j_1, j_2) must be a *multivalued* function of (h,j). The map which relates the original cell to the one obtained after completing the loop is called the monodromy map. It is given by the matrix of the kind $\begin{pmatrix} 1 & -k \\ 0 & 1 \end{pmatrix}$ where k is the number of pinches of the singular fiber $\mathcal{EM}^{-1}(h,j)_{\rm crit}$; in our case $k=1$.

The above concept of monodromy can be naturally transferred to quantum mechanics where in accordance with the EBK quantization principle we should select regular 2-tori (h,j) which have integer values of actions (j_1, j_2). $\mathcal{EM}$ images of such EBK tori form a two-dimensional lattice (see Fig. 6) which can always be smoothly deformed locally into a rectangular lattice (using appropriate local actions). At the same time, the critical value $(h,j)_{\rm crit}$ of $\mathcal{EM}$ is a *point defect* of this lattice.

G. Semi-quantum description, topological quantum numbers

The idea of distinguishing "slow" and "fast" dynamical subsystems described by different dynamical variables $\mathbf{L}_2$ and $\mathbf{L}_1$ respectively leads to the semi-quantum approach where "slow" motion is described using classical mechanics while "fast" motion remains purely quantum. We describe the classical subsystem using a phase space P and associate one or several quantum states with every point $x \in P$ of this space. Each quantum state is characterized by its energy $E_n(x)$ and by corresponding quantum wavefunction $|\psi_n(x)\rangle$. We consider the case when the space P is compact and n runs over a discrete finite set of values. Then with each quantum state n we associate the "energy band" P_n. (The terminology comes from the restriction on the values of the energy function $|E_n(x)| < M < \infty$ for all x in the compact space P; it can also be noted that the quantum spectrum in this case is discrete.) Mathematically P_n is a complex line bundle with base space P and fiber $|\psi_n(x)\rangle$, a complex wavefunction defined over each point x of P. The (possibly nontrivial) topology of this complex line bundle can be characterized by an integer number called the first Chern class which is the topological quantum number of the band P_n. As long as P_n remains isolated (the band has no contact with other bands $P_{n'}$) this topological number is conserved [3].

In the simple situation of $2\mathbf{L}|_{\rm SO(2)}$ the phase space P is a 2-sphere S_2 associated with the $\mathbf{L}_2$ motion, the amplitude of $\mathbf{L}_1$ is fixed and the multiplicity index n runs over a discrete finite set of $2l_1+1$ values. The general solution for the energy function E_n of the Hamiltonian (3) is given in Ref. [2]. In the small γ limit, the Chern numbers C_n for all bands P_n are zero, and the number of states in each band equals $2l_2+1$. In the limit $\gamma \sim 1$, Chern numbers of each band are different. In this limit, the number of states $\mathcal{N}_n$ in band P_n and the Chern number C_n are related as $\mathcal{N}_n = (2j+1-C_n)$. Figure 3 illustrates the case of two bands ($l_1 = \frac{1}{2}$) whose maximum and minimum energy is indicated by dashed lines. As the value of γ increases and comes to $\gamma = 1/2$, the bands connect and at the same time one quantum energy level is transfered from the lower band to the upper band. The connection of the bands corresponds to an isolated conical intersection point of two classical energy functions E_n over S_2. Chern indices of both bands equal 0 when $\gamma < \frac{1}{2}$, and 1 and -1 for the lower and upper band respectively when $\gamma > \frac{1}{2}$. The classical $2\mathbf{L}|_{\rm SO(2)}$ system has monodromy in an interval of parameter values which contains $\gamma = \frac{1}{2}$, and which shrinks to that value in the limit $L_2 \gg L_1$, i.e., for the classical analogue of Fig. 3.

III. SYSTEM WITH THREE COUPLED ANGULAR MOMENTA ($3\mathbf{L}|_{\rm SO(3)}$)

We now consider a system of three coupled angular momenta $\mathbf{L}_1$, $\mathbf{L}_2$, and $\mathbf{L}_3$ in the presence of the SO(3) symmetry. We further assume that components of different momenta Poisson commute and the three amplitudes $L_i = |\mathbf{L}_i|$ are conserved. Due to the SO(3) invariance, our system has two Poisson commuting integrals of motion, the amplitude J of the total angular momentum $\mathbf{J} = \mathbf{L}_1 + \mathbf{L}_2 + \mathbf{L}_3$ and one of the components of $\mathbf{J}$. Since

$$\mathbf{J}^2 = \mathbf{L}_1^2 + \mathbf{L}_2^2 + \mathbf{L}_3^2 + 2[(\mathbf{L}_1\mathbf{L}_2) + (\mathbf{L}_2\mathbf{L}_3) + (\mathbf{L}_3\mathbf{L}_1)],$$

the quantity K,

$$K = \tfrac{1}{2}\left(J^2 - L_1^2 - L_2^2 - L_3^2\right),$$

can serve as an integral of motion instead of J.

To describe unambiguously a system of three vectors in the presence of the SO(3) symmetry, i.e., to specify a configuration of these vectors up to any rotation of the coordinate frame about the origin, we should define three angles between the vectors and introduce an auxiliary variable which distinguishes "left" and "right" orientations. The angles and the orientation can be defined using three scalar products $\tilde{X}_k = (\mathbf{L}_i \cdot \mathbf{L}_j)$, where (ijk) is a cyclic permutation of (123), and the mixed product $\tilde{Y} = (\mathbf{L}_1 \cdot [\mathbf{L}_2 \wedge \mathbf{L}_3])$ respectively [24]. We can see in Fig. 1 that this construction is similar to the $2\mathbf{L}|_{\rm SO(2)}$ case where the third vector is $\mathbf{e}$. If we extend SO(3) by adding simultaneous inversion of the three vectors as a symmetry operation, the mixed product $\tilde{Y}$ will no longer be necessary since "left" and "right" become equivalent. Inversion of angular momenta is achieved by time reversal $\mathcal{T}$, the group $\mathrm{SO(3)} \times \mathcal{T}$ is isomorphic to O(3).

An arbitrary SO(3) invariant Hamiltonian can be written as a polynomial expansion in $\tilde{X}_1$, $\tilde{X}_2$, $\tilde{X}_3$, and $\tilde{Y}$ [25], and in the case of the extended symmetry $\mathrm{SO}(3)\times\mathcal{T}$ the Hamiltonian does not depend on $\tilde{Y}$. In this paper we use a simple one-parameter family of Hamiltonians

$$H_\alpha = \alpha(\mathbf{L}_1\cdot\mathbf{L}_2) + (1-\alpha)(\mathbf{L}_1\cdot\mathbf{L}_3), \tag{5}$$

to illustrate our brief general analysis. This family describes recoupling of three angular momenta which is often encountered in physical systems. In atoms, where spin and angular momentum of the electron(s) are coupled to the spin of the nucleus, the two limits of (5) with $\alpha = 0$ and $\alpha = 1$ represent two different Hund's coupling cases. Many other examples can be easily drawn from molecular physics.

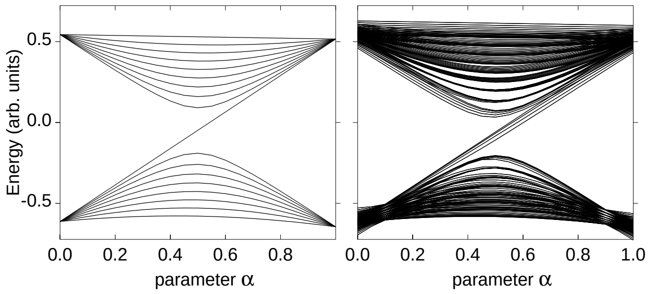

FIG. 7: Energy level spectrum of the model Hamiltonian (5) with $l_1 = \frac{1}{2}$, $l_2 = 4$, and $l_3 = 8$ (left) and of the perturbed Hamiltonian with broken SO(3) symmetry (right). On the left each line corresponds to a j-band of degenerate levels, on the right this degeneracy is removed; the j-bands are further grouped into two "superbands".

IV. REDISTRIBUTION OF BANDS IN QUANTUM SPECTRUM

The quantum spectrum of the $3\mathbf{L}|_{\mathrm{SO}(3)}$ system introduced in Sec. III can be computed straightforwardly. For given fixed amplitudes $|\mathbf{L}_1|$, $|\mathbf{L}_2|$, and $|\mathbf{L}_3|$, the space of quantum wave functions is of dimension $(2l_1+1)(2l_2+1)(2l_3+1)$, where l_1, l_2, and l_3 are respective quantum numbers [16]. Each quantum state can also be chosen as an eigenstate of operators $\mathbf{J}$ and J_z which correspond to the two strict integrals of motion of the system. The $2j+1$ states with the same quantum number j and different projections j_z are degenerate. We call a j-band the group of degenerate levels with the same j. Such j-bands can be in turn assembled into "superbands". Existence and structure of superbands depends on the concrete Hamiltonian.

The superbands of a system with Hamiltonian (5) are associated with additional approximate (or "good") quantum numbers. If α in Eq. (5) is close to zero the amplitude of the angular momentum $\mathbf{J}_{13} = \mathbf{L}_1 + \mathbf{L}_3$ is nearly conserved and j_{13} serves as a good quantum number. Otherwise, when α in Eq. (5) is close to 1, we can use the quantum number j_{12} of the angular momentum $\mathbf{J}_{12} = \mathbf{L}_1 + \mathbf{L}_2$. We can further simplify the situation by assuming that the amplitude of one of the momenta, say $\mathbf{L}_1$, is much smaller than that of two others and also smaller than the module of their difference:

$$l_1 < l_2, \quad l_1 < l_3, \quad l_1 < |l_2 - l_3|.$$

In this case the spectrum of the Hamiltonian (5) in both limits $\alpha\approx 0$ and $\alpha \approx 1$ consists of $2l_1+1$ "superbands" formed by a number of degenerate j-bands. The number of superbands in two limiting cases is the same, $2l_1+1$, but the number of bands within each superband is different.

The energy level spectrum of H_α with $l_1 = \frac{1}{2}$ has two superbands illustrated in Fig. 7 where two other momenta are chosen $l_2 = 4$ and $l_3 = 8$. At small α the superbands in Fig. 7 are characterized by quantum numbers $j_{13} = 7.5$ and $j_{13} = 8.5$, at large $\alpha \approx 1$ we use $j_{12} = 3.5$ and $j_{12} = 5.5$. In the limit $\alpha \approx 0$ each superband includes nine j-bands with $j_{13} - l_2 \le j \le j_{13} + l_2$. When α is close to 1, the two superbands have different number of j-bands with $l_3 - j_{12} \le j \le j_{12} + l_3$.

Comparing Fig. 7, left, to Fig. 3 and similar figures in Refs. [1, 2] shows convincingly that recoupling of three angular momenta in the presence of the SO(3) symmetry is very similar to recoupling of two angular momenta in the presence of the SO(2) symmetry. The main difference is that instead of redistribution of a single energy level (or a group of a fixed number of levels) between j-bands we observe redistribution of j-bands between superbands. To see this latter phenomenon more clearly it is sufficient to break slightly the SO(3) symmetry as shown in Fig. 7, right. Symmetry breaking removes the strict degeneracy of levels within each j-band but redistribution of bands persists because it is a topologically stable phenomenon. Another important difference from $2\mathbf{L}|_{\mathrm{SO}(2)}$ is the internal dynamical degeneracy of bands. Thus for instance, the total number of states in superbands can be different even when the number of bands is the same. The two superbands in Fig. 7 have 144 and 162 states when $\alpha \approx 0$ and 170 and 136 states when $\alpha \approx 1$. When α changes from 0 to 1 one j-band with $j = 12\frac{1}{2}$ is transfered from the lower to the upper superband.

V. CLASSICAL MECHANICAL ANALYSIS

The values L_1, L_2, and L_3 play the role of parameters which give rise to a great variety of classical $3\mathbf{L}|_{\mathrm{SO}(3)}$ systems. We present below a general classification of $3\mathbf{L}|_{\mathrm{SO}(3)}$ systems which is based on symmetry reduction and geometric analysis of the reduced system rather than on the account of any specific features which can be due to a particular Hamiltonian. The example system with Hamiltonian Eq. (5) is studied later in Sec. VI.

A. Phase space and first integrals

A classical mechanical $3\mathbf{L}|_{SO(3)}$ system has three degrees of freedom. Its phase space is a direct product of three 2-spheres $S_2 \times S_2 \times S_2$. The values of L_1, L_2, and L_3, define the radii of the spheres.

The $3\mathbf{L}|_{SO(3)}$ system has two first integrals imposed by the continuous symmetry SO(3) which we call momenta. They define the length J and the orientation of the total angular momentum $\mathbf{J}$. For our subsequent algebraic and geometric analysis the quantity

$$K = \mathbf{L}_2 \cdot \mathbf{L}_3 + \mathbf{L}_1 \cdot \mathbf{L}_3 + \mathbf{L}_1 \cdot \mathbf{L}_2 = \tilde{X}_1 + \tilde{X}_2 + \tilde{X}_3,$$

which is a Casimir of the Poisson algebra generated by $(\tilde{X}_1, \tilde{X}_2, \tilde{X}_3, \tilde{Y})$, is most convenient. On the other hand, analysis of the energy–momentum map in Sec. VI and comparison to quantum mechanics are easier in terms of J. Of course, using K is equivalent to using J^2, see Sec. III. The range of possible values of K and J is defined by the values of L_1, L_2, and L_3.

The other first integral can be any projection of $\mathbf{J}$ [direct computation verifies that $(\mathbf{J} \cdot \mathbf{e})$ Poisson commutes with $\tilde{X}_1$, $\tilde{X}_2$, $\tilde{X}_3$, and $\tilde{Y}$ for any $\mathbf{e}$] and we use $J_z = \mathbf{J} \cdot \mathbf{e}_z$. This integral is not in the algebra of the SO(3) invariants. It characterizes internal structure of the orbits of the SO(3) group action and is not used in the analysis of the reduced system (where these orbits become points on the reduced phase space) but is, of course, required for the reconstruction of invariant tori in the full phase space and for the energy–momentum map. The values of J_z lie in the range $-J, \ldots, J$. By mapping constant level sets of J and J_z in $S_2 \times S_2 \times S_2$ to points in R_2 with coordinates (j, j_z) or (k, j_z), we obtain domains shown Fig. 8.

With three degrees of freedom and two first integrals J (or K) and J_z the $3\mathbf{L}|_{SO(3)}$ system is Liouville integrable. All regular dynamically invariant subspaces of the $S_2 \times S_2 \times S_2$ phase space are 3-tori. Qualitatively different $3\mathbf{L}|_{SO(3)}$ systems have different dynamically invariant singular subspaces.

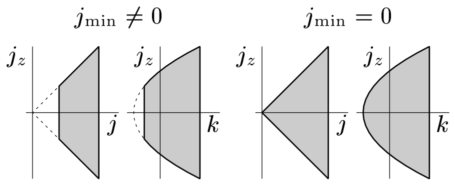

FIG. 8: Image of the momentum map of the $3\mathbf{L}|_{SO(3)}$ system.

B. Group action and orbit space

To describe concisely the action of the symmetry group SO(3) on $S_2 \times S_2 \times S_2$ for all possible (nonzero) values of L_1, L_2, and L_3 we use normalized principal invariant polynomials $X_k = \tilde{X}_k (L_i L_j)^{-1}$,

$$X_1 = \frac{\mathbf{L}_2 \cdot \mathbf{L}_3}{L_2 L_3}, \quad X_2 = \frac{\mathbf{L}_3 \cdot \mathbf{L}_1}{L_3 L_1}, \quad X_3 = \frac{\mathbf{L}_1 \cdot \mathbf{L}_2}{L_1 L_2},$$

and the auxiliary polynomial

$$Y = \tilde{Y}\,(L_1 L_2 L_3)^{-1} = \mathbf{L}_1 \cdot (\mathbf{L}_2 \wedge \mathbf{L}_3)\,(L_1 L_2 L_3)^{-1},$$

which depends algebraically on the X's,

$$\begin{aligned} Y^2 &= \det \begin{vmatrix} \mathbf{L}_1 \cdot \mathbf{L}_1 & \mathbf{L}_1 \cdot \mathbf{L}_2 & \mathbf{L}_1 \cdot \mathbf{L}_3 \\ \mathbf{L}_2 \cdot \mathbf{L}_1 & \mathbf{L}_2 \cdot \mathbf{L}_2 & \mathbf{L}_2 \cdot \mathbf{L}_3 \\ \mathbf{L}_3 \cdot \mathbf{L}_1 & \mathbf{L}_3 \cdot \mathbf{L}_2 & \mathbf{L}_3 \cdot \mathbf{L}_3 \end{vmatrix} (L_1 L_2 L_3)^{-2} \\ &= 1 + 2X_1 X_2 X_3 - X_1^2 - X_2^2 - X_3^2. \end{aligned}$$

Each orbit of the SO(3) action is characterized by (x_1, x_2, x_3), the values of X_1, X_2, and X_3, and the sign of y, the value of Y, and represents uniquely a configuration of the vector triplet $(\mathbf{L}_1, \mathbf{L}_2, \mathbf{L}_3)$ as described in Sec. III. The mixed product Y is nonzero for all generic configurations, it vanishes for all planar and collinear configurations. Two regular orbits of the SO(3) action with the same $|y| \neq 0$ become one orbit of the SO(3) $\times\, \mathcal{T}$ action.

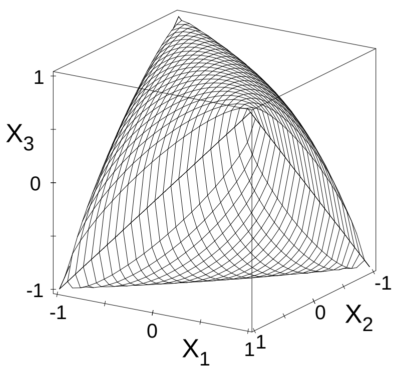

FIG. 9: Orbit space $\mathcal{O}$ of the SO(3) $\times\, \mathcal{T}$ group action on $S_2 \times S_2 \times S_2$ parametrized by the values of three normalized scalar products.

The space of all orbits of the SO(3) $\times\, \mathcal{T}$ action or the *orbifold* $\mathcal{O}$ can be constructed in the ambient space R_3 with coordinates (x_1, x_2, x_3). Orbits with $y = 0$ lie on a closed pillow-like surface which is defined in this space by equation $Y^2 = 0$ (see Fig. 9) and is the familiar puffed tetrahedron described in Sec. II D and Refs. [2, 4, 17, 18]. Indeed, up to replacement of invariants (X_1, X_2, X_3), K, and Y for $(L_{1e} L_1^{-1}, L_{2e} L_2^{-1}, \xi (L_2 L_1)^{-1})$, J_e, and σ, the defining equation of this surface is the same. Geometrically the orbit spaces of the $2\mathbf{L}|_{SO(2)}$ and $3\mathbf{L}|_{SO(3)}$ systems are equivalent but stabilizers of orbits in the case of $3\mathbf{L}|_{SO(3)}$ are, of course, larger. The four vertices of $\mathcal{O}$ correspond to the four collinear configurations of $(\mathbf{L}_1, \mathbf{L}_2, \mathbf{L}_3)$ while other surface points correspond to planar configurations. To learn more on the similarity and difference between $2\mathbf{L}|_{SO(2)}$ and $3\mathbf{L}|_{SO(3)}$ compare the orbits of the two group actions listed in Table I.

TABLE I: Inverse image of points p of the orbifold $\mathcal{O}$ in the case of $\mathrm{SO}(3)\times\mathcal{T}$ and $\mathrm{SO}(2)\times Z_2$ group actions on $S_2\times S_2\times S_2$ and $S_2\times S_2$ respectively.

point $p\in\mathcal{O}$	image of p in $S_2\times S_2\times S_2$	image of p in $S_2\times S_2$
vertices	sphere S_2	point
surface	real projective space RP_3	circle S_1
interior	disjoint union of *two* RP_3	disjoint union of *two* S_1

C. Regular and singular reduced phase spaces

The integral K (or J^2) is a linear function of principal polynomial invariants,

$$K = L_2L_3\,X_1 + L_3L_1\,X_2 + L_1L_2\,X_3,$$

where fixed values of amplitudes (L_1, L_2, L_3) can be regarded as parameters. Constant level sets of K (and J) are planes in the 3-space with normalized coordinates (x_1, x_2, x_3). Intersections V_k of these planes and the orbit space $\mathcal{O}$ are *images* of the reduced phase spaces P_k. If we define coordinates $\chi_1(X,k)$ and $\chi_2(X,k)$ on the constant level plane of K then the phase space P_k can be realized as a closed surface in an ambient 3-space with coordinates (χ_1, χ_2, y). Similar construction is used in Refs. [4, 18] for the $\mathbf{2L}|_{\mathrm{SO}(2)}$ system where the image plane is always parallel to axis ξ (which is now x_3). The $\mathbf{3L}|_{\mathrm{SO}(3)}$ case is much richer because all different planar sections of the orbifold are possible.

TABLE II: Possible critical (or singular) planar sections V_k of the orbit space $\mathcal{O}$ for the SO(3) symmetric system with three angular momenta.

notation	topology of singular section	
g	generic point on the surface ($y=0$) of $\mathcal{O}$	$\circ$
s	singular point, one of the vertices of $\mathcal{O}$	$\bullet$
r	line on the surface of $\mathcal{O}$ connecting two vertices	$\bullet\!\!-\!\!\bullet$
1	closed disk with one singular point on the border	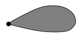
2	closed disk with two singular points on the border	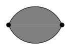
3	closed disk with three singular points on the border	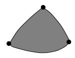

1 Topology of reduced phase spaces

As in the $\mathbf{2L}|_{\mathrm{SO}(2)}$ case [1, 18], the spaces P_k can be regular or singular depending on the value of K. The singularities are caused by the four singular points (vertices) of $\mathcal{O}$. To classify possible reduced phase spaces P_k we consider all possible planar sections V_k of the orbit space $\mathcal{O}$ in Fig. 9. All regular sections V_k have a topology of a closed disc with border S_1. This topology does not change if the variation of k is sufficiently small. Corresponding regular spaces P_k are diffeomorphic to a 2-sphere S_2 (see examples in [4, 18]). All critical (singular) sections V_k either contain one or more vertices or lie in the constant K plane which is tangent to $\mathcal{O}$. Topology of these sections is summarized in Table II. For point sections s, we can distinguish a special case s^* where the point at which the section plane is tangent to $\mathcal{O}$ is a vertex.

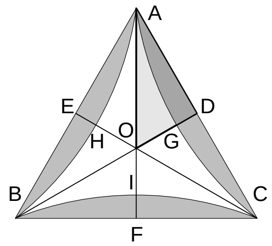

FIG. 10: Regions in the parameter space $L_1{:}L_2{:}L_3$ which correspond to different ratios of angular momenta and qualitatively different sets of singular sections V_k of the orbit space $\mathcal{O}$.

2 Families of reduced phase spaces

The ratio $L_1{:}L_2{:}L_3$ defines orientation of the constant level plane of K, which in turn defines entirely a continuous family of sections V_k and the corresponding family of spaces P_k. The maximum and minimum value of k (and j) is defined by concrete L_1, L_2, and L_3. The parameter space of all possible ratios $L_1{:}L_2{:}L_3$ where at least one of L_i is nonzero, i.e., for $J\neq 0$, can be represented as an equilateral triangle shown in Fig. 10. Vertices, sides, and interior points of this triangle correspond to configurations where two, one, and zero momenta respectively are infinite. With no loss of generality we can choose $0 < L_1 \le L_2 \le L_3$ and consider only the points $L_1{:}L_2{:}L_3$ of the small triangle AOD.

Each possible continuous family of sections V_k and corresponding spaces P_k, where k (and j) takes all possible values for given L_1, L_2, and L_3, is represented by a point of AOD and can be characterized by listing all critical members (singular spaces) of the family. All qualitatively different families are presented in this way in Table III. Obviously, this classification is independent on the concrete $\mathbf{3L}|_{\mathrm{SO}(3)}$ Hamiltonian.

The number of qualitatively different $\mathbf{3L}|_{\mathrm{SO}(3)}$ systems is large in comparison to that of the $\mathbf{2L}|_{\mathrm{SO}(2)}$ systems. The latter can be either a $s11s$ family with $L_1\neq L_2$ studied in [2] or an exceptional $s2s$ family with $L_1 = L_2$ studied on the example of the hydrogen atom in crossed fields [4]. Indeed, while the $\mathbf{2L}|_{\mathrm{SO}(2)}$ orbifold is the same, the integral $J_e = L_{1e} + L_{2e}$ is equivalent to a combination of x_1 and x_2 and the constant level plane of J_e (the plane of V_k) is parallel to x_3. The equivalent $\mathbf{3L}|_{\mathrm{SO}(3)}$ system

TABLE III: Families of planar sections V_k of the orbit space $\mathcal{O}$ of the $\mathbf{3L}|_{\mathrm{SO(3)}}$ system represented by points of the triangle AOD in Fig. 10. The amplitudes are chosen so that $0 < L_1 \leq L_2 \leq L_3$.

region	amplitudes L_1:L_2:L_3	family
O	$0 < L_1 = L_2 = L_3$	$g3s$
A	$0 < L_1, \quad L_2 = \infty, \quad L_3 = \infty$	rr
D	$0 < L_1 = L_2, \quad L_3 = \infty$	$s2s$
G	$0 < L_1 = L_2, \quad L_3 = L_1 + L_2$	s^*2s
AD	$0 < L_1 < L_2, \quad L_3 = \infty$	$s11s$
DG	$0 < L_1 = L_2 < \frac{1}{2}L_3 < \infty$	$s2s$
OG	$0 < L_1 = L_2 < L_3 < 2L_1$	$g12s$
AO	$0 < L_1 < L_2 = L_3$	$g21s$
AG	$0 < L_1 < L_2, \quad L_3 = L_1 + L_2$	s^*11s
AGD	$0 < L_1 < L_2, \quad L_1 + L_2 < L_3 < \infty$	$s11s$
AOG	$0 < L_1 < L_2 < L_3 < L_1 + L_2$	$g111s$

has $L_3 = \infty$ and $L_1 \geq L_2 > 0$ (all points on the AD line in the L_1:L_2:L_3 parameter space in Fig. 10).

3 Reconstruction and number of states diagrams

To describe the dynamics of the initial system we should reconstruct the constant level set of J (or K) in the initial phase space $S_2 \times S_2 \times S_2$. This set is a fiber bundle M_J whose base is the reduced phase space P_k. Even though for all regular values of K the base space has the same S_2 topology, the topology of M_J can be different [20]. Singular members of the family of spaces P_k separate bundles M_J of different topology.

Important physical implications of singular spaces in different families in Table III can be well illustrated by the number of states diagrams similar to the diagram of the $\mathbf{2L}|_{\mathrm{SO(2)}}$ system in Sec. II E. To express the number $\mathcal{N}$ of quantum states with given L_1, L_2, L_3 as function of the amplitude J of the total angular momentum (or K) we should consider all possible coupled quantum states $\big[(L_1, L_2)L_{12}, L_3\big]J$ for each given value j of J. (Recall that the intermediate momentum L_{12} takes integer or half-integer values $|L_1 - L_2|, |L_1 - L_2| + 1, \ldots, L_1 + L_2 - 1, L_1 + L_2$.) The larger dimension of the $\mathbf{3L}|_{\mathrm{SO(3)}}$ system should be taken into account. In order to get piecewise linear continuous diagrams of the same kind as in Sec. II E we should divide the number of states $\mathcal{N}(j)$ by $2j + 1$ (which can be regarded as the number of states associated with the extra degree of freedom). Figure 11 shows $\mathcal{N}(j)/(2j+1)$ diagrams for all qualitatively different families of reduced phase spaces listed in Table III and represented by points L_1:L_2:L_3 of the triangle AOD in Fig. 10. The junction points of the linear pieces of the $\mathcal{N}(j)/(2j+1)$ diagrams (discontinuity points of the first derivative) correspond to singular reduced phase spaces described in Table II.

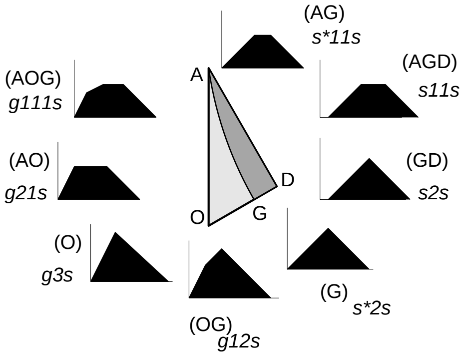

FIG. 11: Normalized number of states as a function of the total angular momentum $\mathcal{N}(j)/(2j+1)$ for all qualitatively different families of reduced phase spaces of the $\mathbf{3L}|_{\mathrm{SO(3)}}$ system which are listed in Table III and defined by the ratio L_1:L_2:L_3 of three coupled angular momenta.

VI. ENERGY MOMENTUM MAP, MONODROMY, REDISTRIBUTION

The image of the energy–momentum map $\mathcal{EM}$ of the $\mathbf{3L}|_{\mathrm{SO(3)}}$ system is a closed domain in R_3 with coordinates (j, j_z, h) or (k, j_z, h). In comparison with the $\mathbf{2L}|_{\mathrm{SO(2)}}$ case in Sec. II F, j_z appears as an extra coordinate which is of little importance because the $\mathbf{3L}|_{\mathrm{SO(3)}}$ Hamiltonian does not depend on it. In other words, J_z stands for an additional internal degree of freedom which is completely uncoupled from the dynamics of the two other degrees.

To find the $\mathcal{EM}$ image for a $\mathbf{3L}|_{\mathrm{SO(3)}}$ system we start with the $J_z = 0$ section of the image. The procedure is similar to that used in Refs. [2, 4] and is based on studying intersections of orbifold sections V_k (or reduced phase spaces P_k) with constant level sets of the Hamiltonian H for all possible k and energies h. We then obtain the whole $\mathcal{EM}$ image by translating its $J_z = 0$ section along axis J_z. In the middle domain, while $j_z \leq j_{\min}$, this gives a parallel prism; for larger j_z we should account for the restriction $|J_z| \leq J$.

A. Examples

In certain cases, such as for the $s11s$ family, we can use the results of Refs. [2, 4] directly. The $\mathbf{3L}|_{\mathrm{SO(3)}}$ system with Hamiltonian (5) can also be analyzed using the results for $\mathbf{2L}|_{\mathrm{SO(2)}}$. In this case we can remark that considering intersections of constant level planes of

$$H = \alpha L_1 L_2 X_3 + (1 - \alpha) L_1 L_3 X_2$$

with sections V_k of the orbifold $\mathcal{O}$ is entirely equivalent to studying intersections of constant level planes of K with orbifold sections V_α (intersections of $\mathcal{O}$ and level planes of H). Of course, the $\mathcal{EM}$ image remains the same (up to a reflection) both in the (h, j) and (j, h) coordinates. In particular, in a certain domain of the values of L_1, L_2, L_3, and α, the $J_z = 0$ slice of the $\mathcal{EM}$ map image of the

$\mathbf{3L}|_{\mathrm{SO(3)}}$ system with Hamiltonian (5) should look like the one in Fig. 6, i.e., the $\mathcal{EM}$ map should have a critical value isolated in the $J_z = 0$ plane. When the $J_z = 0$ slice is translated to other levels of J_z the singular point is *continued* forming a string of singular values in the domain of regular values of the $\mathcal{EM}$ map. The "ends" of the string come out to the boundary of the $\mathcal{EM}$ image.

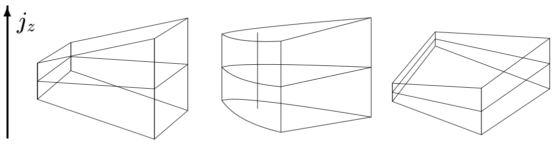

FIG. 12: Schematic three-dimensional images of the energy-momentum map of different possible $\mathbf{3L}|_{\mathrm{SO(3)}}$ Hamiltonians. The central image has an isolated line of singular values of the $\mathcal{EM}$ map and the corresponding system has monodromy.

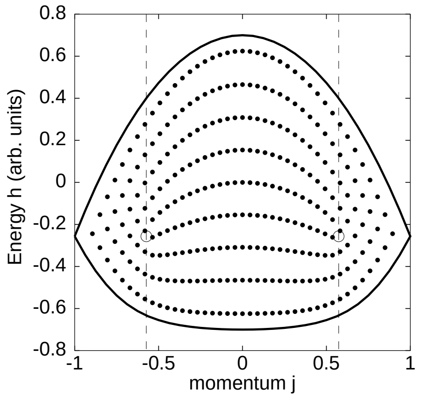

FIG. 13: Image of an energy-momentum map $\mathcal{EM}$ with two isolated critical values projected on the (j, h) plane.

B. General case

The above description illustrates the general situation. Singular values of the $\mathcal{EM}$ map of any $\mathbf{3L}|_{\mathrm{SO(3)}}$ system are due to the four singular points of the orbifold $\mathcal{O}$. Continued in J_z the $\mathcal{EM}$ map image of these points forms strings which can traverse the internal open domain of the regular values of the $\mathcal{EM}$ map but should begin and end on the boundary of that domain. Alternatively, these strings stay on the boundary. A schematic view of the image of the $\mathcal{EM}$ map for some different possible $\mathbf{3L}|_{\mathrm{SO(3)}}$ Hamiltonians is given in Fig. 12. Left and right images on this figure correspond to the situation where singular values of the $\mathcal{EM}$ map lie on the boundary. In this case, action-angle variables are well defined globally. The $\mathcal{EM}$ map image in the center of Fig. 12 has a line of singular values surrounded by regular values. In each $J_z = \mathrm{const}$ slice of this image (which cuts the singular line) the isolated singular value prohibits global action-angle variables precisely in the same way as in the $\mathbf{2L}|_{\mathrm{SO(2)}}$ case described in Sec. II F and Fig. 6. Such $\mathbf{3L}|_{\mathrm{SO(3)}}$ system has classical and quantum monodromy.

The central image in Fig. 12 presents the simplest $\mathbf{3L}|_{\mathrm{SO(3)}}$ system with monodromy. Other systems can have two or even three strings of isolated critical values of $\mathcal{EM}$ which traverse the domain of regular values. An image of the quantum and classical $\mathcal{EM}$ map of such system is shown in Fig. 13. We can see that monodromy for the loop around either of the two isolated critical values in this figure equals $+1$, while monodromy for the loop around both values equals $+2$. This illustrates the general case for holonomic Hamiltonian systems where monodromies of several isolated critical values which lie in the *same* domain of regular values of the $\mathcal{EM}$ map have the same "sign" and obey the "sum rule".

C. Quantum monodromy, redistribution

If we look at the central $\mathcal{EM}$ map image in Fig. 12 "from the top", i.e., if we average the $\mathcal{EM}$ map over the internal dynamical variable J_z or simply project the $\mathcal{EM}$ map image on the (h, j) plane, we can use Fig. 6 to analyze the quantum $\mathbf{3L}|_{\mathrm{SO(3)}}$ system bearing in mind that each black dot in this figure now represents a "band" of $2j+1$ quantum states with $j_z = -j, \ldots, j$ rather than an individual level. Like in the $\mathbf{2L}|_{\mathrm{SO(2)}}$ case, the lattice of quantum bands has a "defect" or quantum monodromy when it has an isolated singular point surrounded by regular points.

The lattice of quantum bands of our example Hamiltonian (5) with parameter α set to $\frac{1}{2}$ has precisely the defect described above. It should be remarked that in order to observe this defect we should be sufficiently close to the classical limit of large L_1, L_2, and L_3. Thus, in the case of the quantum system shown in Fig. 7, left, the ratio L_1:L_2:L_3 should be kept L:$8L$:$16L$ but L should be large enough to have many bands (many points in the lattice). If, on the other hand, we are at the opposite limit of the smallest possible $L = \frac{1}{2}$ (Fig. 7, left), then the monodromy of the system manifests itself as a redistribution of a band between the two superbands which occurs when parameter α is varied near $\frac{1}{2}$.

It follows that, like in the $\mathbf{2L}|_{\mathrm{SO(2)}}$ case [2], we can understand monodromy of the $\mathbf{3L}|_{\mathrm{SO(3)}}$ system with Hamiltonian (5) either by taking a truly classical limit of large L or by considering a one-parameter family of Hamiltonians. There is, however, an important difference between the $\mathbf{2L}|_{\mathrm{SO(2)}}$ and $\mathbf{3L}|_{\mathrm{SO(3)}}$ system. In the former case, a fixed number of levels is redistributed between the two bands (in the example of [2] this number is one, but it can be larger in the presence of some finite symmetry group). In particular, this number does not change as we approach the classical limit of large L. On the other hand, the number of levels in the band which is redistributed between the two superbands of the $\mathbf{3L}|_{\mathrm{SO(3)}}$ system increases with L.

D. Conclusion

Integrable Hamiltonian dynamical systems with more than two degrees of freedom may have complex topological obstructions to the existence of global action-angle variables. Though predicted theoretically [9] such obstructions have never been identified in concrete systems. Thus we should conclude that in spite of its increased dimension, the $3\mathbf{L}|_{\mathrm{SO}(3)}$ system has the same monodromy as the $2\mathbf{L}|_{\mathrm{SO}(2)}$ system, i.e., of the simplest kind known in two degrees of freedom. The reason for such similarity between the two systems is in the symmetry group action which in both systems has the same orbit space $\mathcal{O}$.

VII. SEMI-QUANTUM DESCRIPTION

Out of several possible semi-quantum $3\mathbf{L}|_{\mathrm{SO}(3)}$ systems we take the one with two classical angular momenta and one quantum : we suppose that the dynamical variables associated with $\mathbf{L}_1$ can be considered as "fast" and all others as "slow". The fast dynamics is described using quantum mechanics; slow variables are made classical. The semi-quantum Hamiltonian $\hat{H}$ of the $3\mathbf{L}|_{\mathrm{SO}(3)}$ system is a matrix of dimension $2L_1+1$ defined on the four-dimensional classical phase space $S_2\times S_2$ of the slow variables. The minimum number of two quantum states ($L_1 = \frac{1}{2}$) suffices the study of level redistribution (see Fig. 7, left).

The eigenvalues of the matrix $\hat{H}$ are classical Hamiltonians (energy functions) describing the internal structure of each individual quantum state. If these eigenvalues are isolated, i.e., if no degeneracies occur at any accessible point of classical phase space, we speak of distinct bands in the quantum spectrum. If they are isolated for all members $\hat{H}_\alpha$ in a parametric family of Hamiltonians (some deformation of $\hat{H}$), the band structure of the quantum spectrum remains qualitatively the same within the family. Degeneracy of eigenvalues can signal a qualitative change, such as redistribution of levels between the bands. As we already noted above, this phenomenon seems to be closely related to the monodromy of the corresponding entirely classical system.

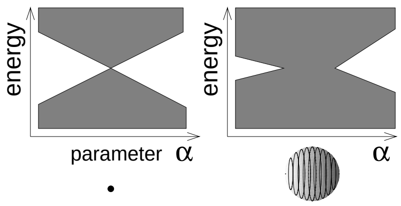

FIG. 14: Typical contact of two bands and corresponding degeneracy manifolds for the one-parameter family of 2×2 Hermitian matrices $\hat{H}_\alpha$ defined over a two-dimensional phase space (left), and over a four-dimensional phase space (right).

A. Degeneracy manifolds

If $\hat{H}$ is defined over a phase space of dimension two (see Fig. 14, left), the eigenvalues are, generically, nondegenerate. Isolated degeneracy points can appear in a one-parameter family $\hat{H}_\alpha$ (two variables plus one control parameter α) [26]. A generic semi-quantum system with two levels and a four-dimensional phase space can have a one-dimensional subspace where its two eigenvalues are degenerate. A one-parameter family $\hat{H}_\alpha$ of such systems should typically have an interval of parameter values where the eigenvalues are degenerate (see Fig. 14, right). The degeneracy manifold is, therefore, a two-dimensional space immersed in an extended space of dimension five (four variables plus one parameter).

Continuous symmetry of $\hat{H}$ changes the situation. Degeneracy on the generic orbit of the group action becomes less possible. In the $2\mathbf{L}|_{\mathrm{SO}(2)}$ case (see Sec. II G) the phase space of $\hat{H}$ is a two-sphere which is further foliated into S_1 orbits of the SO(2) group action. The number of dynamical variables is decreased by one. This makes degeneracy on the generic orbit not typical even in a one-parameter family. However, the eigenvalues of $\hat{H}$ can become degenerate at the critical orbits (fixed points of the SO(2) action on S_2) at an isolated value of parameter.

In the case of the $3\mathbf{L}|_{\mathrm{SO}(3)}$ system, the orbit of the SO(3) action on the $S_2\times S_2$ phase space of $\hat{H}$ is three dimensional. Again, degeneracy appears at an isolated value of the control parameter and at a critical orbit which corresponds to one of the collinear configurations of "slow" $\mathbf{L}_2$ and $\mathbf{L}_3$ and has the topology of a sphere S_2. Breaking the SO(3) symmetry down to SO(2) (Fig. 7, right) splits this one critical SO(3) orbit S_2 into one-dimensional SO(2) orbits S_1 but at the same time makes it possible for the degeneracy to exist at different SO(2) orbits for different values of the control parameter. Such symmetry breaking preserves the S_2 topology of the degeneracy manifold in the extended space (phase space extended by the control parameter).

The topology of the degeneracy manifold is an important characteristics of the redistribution phenomenon. When this manifold is a point (Fig. 14, left) a single quantum state is redistributed between the two groups of states or branches; when it is a sphere (Fig. 14, right), an entire band (branch) of $2j+1$ levels is transferred between the groups which are now called superbands. This transfer can be described using topological quantum numbers as it was done for the $2\mathbf{L}|_{\mathrm{SO}(2)}$ system in Sec. II G and Ref. [3].

B. Chern indices

In the simplest case with quantum angular momentum $L_1 = \frac{1}{2}$ illustrated in Fig. 7, the semi-quantum Hamiltonian $\hat{H}_\alpha$ is a 2×2 matrix defined over the phase space

$S_2 \times S_2$. Two quantum wavefunctions associated with each point of $S_2 \times S_2$ form a complex vector bundle of rang 2. This bundle can be decomposed into two line bundles which correspond to two superbands of the quantum spectrum. Since the base space $S_2 \times S_2$ is a direct product of two manifolds, we should use two first Chern classes c_1 and d_1 to characterize the topology of the line bundles. Thus, the two line bundles originating from a trivial vector bundle of rang 2 over $S_2 \times S_2$ have first Chern classes (c_1, d_1) and $(-c_1, -d_1)$. The superband corresponding to the line bundle (c_1, d_1) has $(2l_2 + 1 - c_1)(2l_3 + 1 - d_1)$ states. In the absence of any symmetry and coupling the rang 2 vector bundle is trivial. In the two limits in Fig. 7 this bundle decomposes as follows.

	$\alpha = 0$ limit	$\alpha = 1$ limit
indices (c_1, d_1)	$(\pm 1, 0)$	$(0, \pm 1)$
number of states	$(2l_2)(2l_3 + 1)$	$(2l_2 + 1)(2l_3)$
	$(2l_2 + 2)(2l_3 + 1)$	$(2l_2 + 1)(2l_3 + 2)$

VIII. IS FURTHER GENERALIZATION POSSIBLE?

We have shown in this paper that the phenomenon of the energy level redistribution between branches of the $\mathbf{2L}|_{\mathrm{SO}(2)}$ system can be generalized to the redistribution of whole branches between superbands of the $\mathbf{3L}|_{\mathrm{SO}(3)}$ system. It is natural to ask whether such phenomena can be typical in general semi-quantum systems whose “slow” classical variables are defined over a phase space P of certain dimension and topology?

The “slow” system in our $\mathbf{3L}|_{\mathrm{SO}(3)}$ example has one important particular aspect. This system has two degrees of freedom which can be further separated. Such separation is possible because our “slow” phase space P is a direct product $S_2 \times S_2$. As a consequence, we can introduce an additional good quantum number which characterizes the internal structure of the superband. The number of bands within the superband is conserved for any isolated superband. If the phase space P is not a direct product of simpler spaces, splitting of superbands into branches or subbands cannot be done without further assumptions. The most natural example is a classical phase space CP_k of a reduced $k + 1$ degenerated oscillator.

If the classical phase space P is irreducible (cannot be factorized) no redistribution between two superbands except for a trivial interchange of two superbands can take place. The reason is quite simple. Internal structure of each superband depends, of course, on the concrete Hamiltonian, but the number $\mathcal{N}$ of quantum states in the superband depends only on the quantum number n which labels different superbands. The number of states $\mathcal{N}(n)$ is a polynomial in n whose degree equals $\frac{1}{2}\dim P$, i.e., the number of slow degrees of freedom. The number of states before and after redistribution is described by the *same* polynomial $\mathcal{N}$ but the quantum number n can change. For example, consider two superbands with the same initial number of states $\mathcal{N}(n)$. After redistribution, they have different number of states, $\mathcal{N}(n')$ and $\mathcal{N}(n'')$. Of course, the total number of states is preserved,

$$2\mathcal{N}(n) = \mathcal{N}(n') + \mathcal{N}(n'').$$

Since the above equation has no solution (n, n', n'') when degree of $\mathcal{N}$ is greater than one, any nontrivial redistribution between two bands is impossible.

An exchange between two bands does not, of course, exhaust all possibilities. Thus consider three isolated superbands defined over the classical phase space CP_2 (of real dimension 4) which are all initially labelled by quantum number n. The number of states polynomial $\mathcal{N}(n)$ is quadratic. After the three superbands contact and states are redistributed, one isolated superband with $n' \neq n$ emerges while two others constitute one non-separable “double” superband. Such rearrangement was studied from a formal topological point of view in Ref. [27], physical examples and interpretation remain to be found [28].

ACKNOWLEDGMENTS

This work was supported by the EU project Mechanics and Symmetry in Europe (MASIE), contract no. HPRN-CT-2000-00113. We thank Jean Belissard, Richard Cushman, and Frédérick Faure for discussions.

SPHERICAL MAP OF THE REDUCED PHASE SPACE OF THE $\mathbf{2L}|_{\mathrm{SO}(2)}$ SYSTEM

We show how the phase space and the Poisson algebra of the reduced $\mathbf{2L}|_{\mathrm{SO}(2)}$ system can be mapped to a 2-sphere and a Lie algebra so(3) respectively. For the particular case of the perturbed Kepler problem (hydrogen atom in fields) this map has already been discussed in [4]. Following [4] we redefine basic invariant polynomials,

$$\begin{aligned} \pi_1 &= L_{1e} - L_{2e}, && \text{(6a)} \\ \pi_2 &= 4(\mathbf{L}_1 \cdot \mathbf{L}_2) - 4(L_{1e}^2 + L_{2e}^2), && \text{(6b)} \\ \pi_3 &= 4\big([\mathbf{L}_1 \times \mathbf{L}_2] \cdot \mathbf{e}\big) = 4\sigma, && \text{(6c)} \\ \pi_4 &= L_{1e} + L_{2e}. && \text{(6d)} \end{aligned}$$

Relation (4) for the new polynomials $(\pi_1, \ldots, \pi_4)$ is

$$\pi_2^2 + \pi_3^2 = (2L_2 + \pi_4 - \pi_1)(2L_2 - \pi_4 + \pi_1)(2L_1 + \pi_1 + \pi_4)(2L_1 - \pi_1 - \pi_4) = \mathcal{X}^2_{L_1, L_2, c}\,. \qquad (7)$$

For each fixed value c of the momentum (the conserved quantity) π_4 the reduced phase space $P_{L_1,L_2,c}$ is defined as a surface in R_3 with coordinates (π_1,π_2,π_3) which is symmetric with respect to rotations about axis π_1. The map

$$R_3 \to R_3 : (\pi_1,\pi_2,\pi_3) \to (J_1,J_2,J_3)$$

maps $P_{L_1,L_2,c}$ to a sphere S_2 defined in the space R_3 with coordinates (J_1,J_2,J_3) by the equation

$$J_1^2 + J_2^2 + J_3^2 = J^2.$$

To construct this map explicitly we look for a function $\mathcal{F}_{L_1,L_2,c}(\pi_1) > 0$ such that

$$\pi_2 = J_2\,\mathcal{F}_{L_1,L_2,c}(\pi_1), \quad \pi_3 = J_3\,\mathcal{F}_{L_1,L_2,c}(\pi_1)$$

and

$$\pi_2^2 + \pi_3^2 = (J_1^2 - J^2)\,\mathcal{F}^2_{L_1,L_2,c}(\pi_1), \tag{8}$$

where $J_1(\pi_1)$ is linear in π_1 and $\mathcal{F}_{L_1,L_2,c}(\pi_1)$ is a product of two of the four factors of $\mathcal{X}_{L_1,L_2,c}$ in Eq. (7). Assuming (with no loss of generality) that $L_1 \geq L_2$, the choice of functions $\mathcal{F}_{L_1,L_2,c}(\pi_1)$ and $J_1(\pi_1)$ in each of the three c-value domains is given below.

domain of c values	definition of J_1	definition of $\mathcal{F}_{L_1,L_2,c}$	value of J
$L_1+L_2 \geq c \geq L_1-L_2$	$\frac{1}{2}\left[\pi_1-(L_1-L_2)\right]$	$2\sqrt{(2L_2-\pi_1+c)(2L_1+\pi_1+c)}$	L_1+L_2-c
$L_1-L_2 \geq c \geq L_2-L_1$	$\frac{1}{2}(\pi_1-c)$	$2\sqrt{4L_1^2-(\pi_1+c)^2}$	$2L_2$
$L_2-L_1 \geq c \geq -(L_1+L_2)$	$\frac{1}{2}\left[\pi_1-(L_1-L_2)\right]$	$2\sqrt{(2L_2+\pi_1-c)(2L_1-\pi_1-c)}$	L_1+L_2+c

The value of J (the radius of S_2) in each of the domains is also chosen differently and it can be seen that $J(c)$ is a piecewise linear continuous function. In the case $L_1 = L_2 = \frac{1}{2}n$ of [4] the central domain of c values shrinks to a point and $J(c) = n - |c|$.

In order to find the Poisson algebra generated by (J_1,J_2,J_3) we recall the definition of $(\pi_1,\pi_2,\pi_3,\pi_4)$ in terms of Poisson commuting angular momenta $\mathbf{L}_1$ and $\mathbf{L}_2$ restricted by $\mathbf{L}_1^2 = L_1^2$ and $\mathbf{L}_2^2 = L_2^2$ and find the Poisson algebra generated by (π_1,π_2,π_3). The structure of this algebra is

$$\begin{aligned}
\{\pi_1,\pi_2\} &= 2\pi_3, \\
\{\pi_3,\pi_1\} &= 2\pi_2, \\
\{\pi_3,\pi_2\} &= 4\pi_1\left[\pi_1^2 - 2(L_1^2+L_2^2) - c^2\right] + 8c(L_1^2 - L_2^2).
\end{aligned}$$

Here π_4 is replaced by its value c since $\{\pi_4,\pi_k\} = 0$, for $k = 1,2,3$. We can also remark that function

$$\psi_{L_1,L_2,c}(\pi_1,\pi_2,\pi_3) = \pi_2^2 + \pi_3^2 - \mathcal{X}^2_{L_1,L_2,c}$$

is a Casimir of this algebra and obtain Dirac's formula

$$\{\pi_i,\pi_j\} = \epsilon_{ijk}\frac{\partial\psi}{\partial\pi_k}.$$

To verify that in each of the three c-value domains the Poisson algebra generated by (J_1,J_2,J_3) is a standard Lie algebra so(3) with structure

$$\{J_\alpha,J_\beta\} = \epsilon_{\alpha\beta\gamma}J_\gamma,$$

we compute the bracket

$$\{J_\alpha,J_\beta\} = \sum_{i=1}^{3}\sum_{j=1}^{3}\frac{\partial J_\alpha}{\partial\pi_i}\frac{\partial J_\beta}{\partial\pi_j}\{\pi_i,\pi_j\}$$

and *simplify* the result using relation (7).

REFERENCES

[*] e-mail: zhilin@univ-littoral.fr

[1] V. B. Pavlov-Verevkin, D. A. Sadovskií, and B. I. Zhilinskií. Europhys. Lett. **6** 573 (1988).

[2] D. A. Sadovskií and B. I. Zhilinskií, Phys. Lett. A, **256** 235 (1999). Invariants $(L_{1e}, L_{2e}, \xi, \sigma)$ in Sec. II of the present paper correspond to (S_z, N_z, ξ, σ).

[3] F. Faure and B. Zhilinskií, Phys. Rev. Lett. **85** 960 (2000).

[4] D. A. Sadovskií and R. H. Cushman, Europhys. Lett. **47**, 1 (1999); Physica D **142**, 166 (2000).

[5] Books on atomic spectroscopy; see also Chap. XVI § 121 of Ref. [19]

[6] B. I. Zhilinskií and S. Brodersen, J. Mol. Spectrosc. **163**, 326 (1994); S. Brodersen and B. I. Zhilinskií, J. Mol. Spectrosc. **169**, 1 (1995); **172**, 303 (1995).

[7] D. A. Sadovskií, B. I. Zhilinskií, J.-P. Champion, and G. Pierre, J. Chem. Phys. **92**, 1523 (1990).

[8] D. J. Thouless, *Topological Quantum Numbers in Nonrelativistic Physics* (World Scientific, Singapore, 1998).

[9] J. J. Duistermaat, Comm. Pure Appl. Math. **33**, 687 (1980).

[10] R. H. Cushman and L. M. Bates, *Global aspects of classical integrable systems* (Birkhäuser, Basel, 1997).

[11] L. M. Lerman and Ya. L. Umanskií, *Four dimensional integrable Hamiltonian systems with simple*

singular points (topological aspects). Transl. Mathematical Monographs **176** (AMS, 1998).

[12] L. M. Lerman and Ya. L. Umanskií, Prikl. Mat. Mekh. **47**, 395 (1983); English transl. in J. Appl. Math. Mech. **47** (1983); Russian Acad. Sci. Sb. Math. **77**, 511 (1994); **78**, 479 (1994).

[13] R. H. Cushman and J. J. Duistermaat, Bull. Am. Math. Soc. **19**, 475 (1988).

[14] San Vũ Ngọc, Comm. Math. Phys. **203**, 465 (1999).

[15] M. S. Child, J. Phys. A **31**, 657 (1998); M. S. Child, T. Weston, and J. Tennyson, Mol. Phys. **96**, 371 (1999).

[16] We do not denote differently quantum operators and classical functions, neither do we sophisticate our notation in order to distinguish values of classical functions and quantum numbers (expectation values) of corresponding operators. In most cases, classical values and quantum numbers are denoted by small, while functions and operators—by capital letters; bold letters stand for 3-space vectors. Quantum number l of the angular momentum operator $\mathbf{L}$ takes integer or half-integer values. Since the eigenvalue of the operator $\mathbf{L}^2$ equals $l(l+1)$, the classical amplitude $|\mathbf{L}|$ of the angular momentum $\mathbf{L}$ can be more correctly related to the corresponding quantum number as $|\mathbf{L}| = \sqrt{l(l+1)}$. In the classical limit of large l such definition becomes unimportant. It is often replaced by $|\mathbf{L}| = l + \frac{1}{2}$ or simply by $|\mathbf{L}| = l$.

[17] D. A. Sadovskií, B. I. Zhilinskií, and L. Michel, Phys. Rev. A **53**, 4064 (1996).

[18] L. Michel and B. I. Zhilinskií, Phys. Rep. **341**, 11 (2001); B. I. Zhilinskií, Phys. Rep. **341**, 85 (2001).

[19] L. D. Landau and E. M. Lifshitz, *Quantum mechanics. Non-relativistic theory.* Ser. Theoretical physics, Vol. III, third edition (Moscow, Nauka, 1974). English transl. (Pergamon Press, Oxford, 1965).

[20] J. J. Duistermaat and G. J. Heckman, Invent. Math. **69**, 259 (1982).

[21] V. Guillemin, *Moment Maps and Combinatorial Invariants of Hamiltonian T^n-spaces* (Birkhäuser, Basel, 1994), Chap. 2.

[22] M. Audin, *Topology of Torus Actions on Symplectic Manifolds* (Birkhäuser, Basel, 1991), Chap. 5.

[23] R. H. Cushman and J. J. Duistermaat, J. Diff. Eqns. **172** 42 (2001); *Non-Hamiltonian monodromy* (University of Utrecht, preprint 1997).

[24] H. Weyl, *Classical groups, their invariants and representations* (Princeton University Press, New Jersey, 1939). Weyl treats a general case of configurations of k-vectors in n-dimensions.

[25] More precisely, X_1, X_2, and X_3 are algebraically independent (denominator) invariants and Y is an auxiliary (numerator) invariant. Any invariant function or any invariant polynomial in the multiplicative ring generated by X_1, X_2, X_3, and Y can be expressed using products of arbitrary powers of X's times, possibly, Y. In particular, due to the algebraic dependence between Y and X's of the kind $f(Y^2, X_1, X_2, X_3) = 0$ any power of Y higher than 1 can be expressed in the above manner. Such construction was introduced by Weyl [24], who called it integrity basis. For more details, review of physical applications of the theory of invariants, and relevant references see [18].

[26] The splitting $\sqrt{(a-b)^2 + [\mathrm{Re}(c)]^2 + [\mathrm{Im}(c)]^2}$ of the two eigenvalues of a generic Hermitian matrix $\begin{pmatrix} a & c \\ \bar{c} & b \end{pmatrix}$ vanishes if three independent real quantities become zero, see J. von Neumann and E. Wigner, Phys. Z. **30**, 467 (1929).

[27] L. N. Chang and Y. Liang, Mod. Phys. Letters A, **3**, 1839 (1988).

[28] F. Faure and B. I. Zhilinskií, in preparation.